The prediction of the diffuse field sound absorption of perforated panel systems

David James Larner[1]
John Laurence Davy[2]
RMIT University
GPO Box 2476
Melbourne, VIC 3001 Australia

This paper studies the diffuse field sound absorption coefficient of a system consisting of a rigid perforated panel with a thin porous woven/matted material glued to its back, which is placed in front of an air cavity with a rigid backing. To cut the cost of trial and error diffuse field sound absorption coefficient measurements, a prediction method was developed. Measurements were made in a two-microphone impedance tube of the complex specific acoustic impedances of the un-perforated rigid panel materials, and of the thin porous materials in front of a rigidly terminated air cavity. These values were used in the transfer matrix method to predict the complex specific acoustic impedances of the perorated panels systems as a function of the angle of incidence of the sound. These calculations assumed the systems to have infinite or finite lateral extent. The measured diffuse field absorption values usually lay between the infinite and finite predictions. The most important variables are the perforation factor of the panel, the acoustic resistance of the thin porous material and the cavity depth.

1. INTRODUCTION

Trial and error can be an expensive task when developing new materials for perforated panel systems. To reduce the cost of diffuse field sound absorption measurements, a prediction method for a system consisting of a rigid perforated panel with a thin porous woven or matted material glued to its back, which is placed in front of an air cavity with a rigid backing, has been developed. The complex specific acoustic impedance of the apertures of the perforated panel was calculated by using predictions of the complex characteristic acoustic impedance and complex wavenumber of the apertures of the perforated panel[1], and using the transfer matrix method[2] to add the impedance of the air cavity. The complex specific acoustic impedance of the thin porous material is added to the complex specific acoustic impedance of

[1] david.larner@rmit.edu.au
[2] john.davy@rmit.edu.au

the air cavity, where the perforation ratio of the panel divides the impedance of the thin porous material.

The complex specific impedance of the panel material is placed in parallel with the complex specific impedance of the system, as this material can be absorptive. The infinite radiation impedance was originally used to predict the diffuse field sound absorption. However, this usually under-predicts compared to the measured values. Therefore, the finite radiation impedance was used in the calculation of the diffuse field sound absorption[3]. This method over-predicts the measured values, which means that the average between the infinite and finite analysis can be used as an estimate of the diffuse field sound absorption coefficient.

2. THEORY

2.1 Infinite calculation of the diffuse field sound absorption

Perforated panels have been used as Helmholtz resonators in the sound absorption industry for a number of years. After studying the micro-perforated theory[4-6], the development of a method to predict the diffuse field sound absorption coefficient α of a much thicker panel was instigated. Since the transfer matrix method is used, the specific acoustic impedance of the rigidly terminated air cavity at the back of the holes in the perforated panel needs to be calculated first;

$$Z_{cav} = -jp\rho_0 c \cot(kD\cos\theta) / \cos\theta \quad (1)$$

where p is the perforation ratio of the panel, $\rho_0 c$ is the characteristic impedance of air, k is the wavenumber of air, D is the air cavity depth, and θ is the angle of incidence. The reason for the multiplication of the perforation ratio here is the difference between the acoustic particle velocity inside and outside the holes.

Here, the measured complex specific acoustic impedance of the thin porous material Z_{woven} is added to the impedance of the air cavity.

$$Z_1 = Z_{woven} + Z_{cav} \quad (2)$$

This measurement is performed in both a low frequency and a high frequency two-microphone impedance tube, so a wide range of frequencies are measured (172 – 5936 Hz). This was performed by gluing the material to a metal mount, so the thin porous material is free standing, roughly one-quarter wavelength of the maximum frequency away from the rigid backing. This quarter wavelength-sized air cavity is then subtracted from the measurements, so the complex specific acoustic impedance of the material is solely added to the theoretical air cavity depth.

Before the transfer matrix method is used, the complex characteristic impedance and complex wavenumber of the perforated panel needs to be calculated. These values are calculated using the effective density ρ_e and the bulk modulus K. For circular apertures, the bulk modulus (at 18°C) can be calculated by;

$$K_{cir} = \gamma P_o / \left[1 + (\gamma - 1)\frac{2}{Bs\sqrt{-j}}\frac{J_1(Bs\sqrt{-j})}{J_0(Bs\sqrt{-j})}\right] \quad (3)$$

where γ is the diatomic adiabatic constant, P_o is the ambient mean pressure, B is the square root of the Prandtl number ($\sqrt{0.71}$), and J_n is the nth order Bessel function of the first kind. s is equal to;

$$s = \sqrt{\frac{\omega \rho_0 R^2}{\eta}} \quad (4)$$

where ω is the angular frequency, ρ_0 is the density of air, R is the radius of the aperture, and η is the viscosity of air.

These previous two equations can be modified for slits;

$$K_{slit} = \gamma P_o / \left[1 + (\gamma - 1)\frac{\tanh(Bs\prime\sqrt{j})}{Bs\prime\sqrt{j}}\right] \quad (5)$$

$$s' = \sqrt{\frac{\omega \rho_0 a^2}{\eta}} \quad (6)$$

where a is the width of the slit.

The effective density is then calculated, for both circular apertures $\rho_{e_{cir}}$ and slits $\rho_{e_{slit}}$ respectively;

$$\rho_{e_{cir}} = \rho_0 / \left[1 - \frac{2}{s\sqrt{-j}}\frac{J_1(s\sqrt{-j})}{J_0(s\sqrt{-j})}\right] \quad (7)$$

$$\rho_{e_{slit}} = \rho_0 / \left[1 - \frac{\tanh(s\prime\sqrt{j})}{s\prime\sqrt{j}}\right] \quad (8)$$

From these calculations, the complex characteristic impedance Z_c and complex wavenumber k' of the perforated panel can be calculated;

$$Z_c = \sqrt{K\rho_e} \quad (9)$$

$$k' = \omega\sqrt{\rho_e / K} \quad (10)$$

There needs to be an angular dependent term when calculating the specific acoustic impedance of the apertures in the perforated panel. This is obtained when calculating the component of the vector of the complex wavenumber transmitting in the plane perpendicular to the face of the panel k'_3;

$$k'_3 = \sqrt{k'^2 - {k_0}^2 \sin^2(\theta)} \quad (11)$$

With these values, the specific acoustic impedance of the apertures in the panel Z_0 can now be calculated;

$$Z_0 = \frac{Z_c}{p}\frac{k'}{k'_3}\frac{-jZ_1\cot(k'_3 t) + Z_c\frac{k'}{k'_3}}{Z_1 - jZ_c\frac{k'}{k'_3}\cot(k'_3 t)} \tag{12}$$

where t is the thickness of the panel. To obtain the total impedance of the system, the material impedance of the panel needs to be incorporated into the system. This was performed by first measuring the complex specific acoustic impedance of an un-perforated version of the panel Z_{panel}, rigidly-backed, in the two-microphone impedance tube. These measurements were then used in parallel with the aperture impedances, to give the total impedance of the system;

$$Z_{tot} = \left(\frac{1}{Z_0} + \frac{1-p}{Z_{panel}}\right)^{-1} \tag{13}$$

The diffuse field sound absorption coefficient can then be calculated for the entire system using the commonly found equation;

$$\alpha = 8\int_0^{\frac{\pi}{2}} \sin\theta\cos\theta \frac{Re\left(\frac{Z_{tot}}{\rho_0 c}\right)\cos\theta}{\left[1 + Re\left(\frac{Z_{tot}}{\rho_0 c}\right)\cos\theta\right]^2 + \left[Im\left(\frac{Z_{tot}}{\rho_0 c}\right)\cos\theta\right]^2} d\theta \tag{14}$$

2.2 Finite calculation of the diffuse field absorption

Finite analysis was also used to calculate the diffuse field sound absorption coefficient, as this method tends to boost the diffuse field sound absorption coefficient values across all frequencies. This was performed by calculating the normalized complex finite radiation impedance[3]. Firstly, the real part of the normalized finite radiation impedance must be calculated:

$$Re(z_F) = \left[Re\left(z_{F_H}\right)^{-2} + \left(\frac{{k_0}^2 A}{2\pi}\right)^{-2}\right]^{-\frac{1}{2}} \tag{15}$$

where A is the area of the perforated panel, and the high frequency approximation of the normalized finite impedance z_{F_H} is;

$$z_{F_H} = \sqrt{\left(\cos^2\theta + \left[\frac{\beta(L+W)}{Ak_0}\right]^2 - 2j\frac{\beta(L+W)}{Ak_0}\sin\theta\right)^{-1}} \tag{16}$$

where L and W are the length and width of the perforated panel respectively, and $\beta = 0.956$.

The imaginary part of the normalized radiation impedance is calculated by;

$$Im(z_F) = \begin{cases} z_{F_0} & if\ z_{F_0} > Im(z_{F_H}) \\ Im(z_{F_H}) & if\ \ z_{F_0} < Im(z_{F_H}) \end{cases} \tag{17}$$

where;

$$z_{F_0} = \left[\left(\frac{k_0 \left[WH\left(\frac{L}{W}\right) + L\,H\left(\frac{W}{L}\right) \right]}{\pi} \right)^{-2} + \left(\frac{0.67(L+W)}{k_0 A} \right)^{-2} \right]^{-\frac{1}{2}} \tag{18}$$

and;

$$H(x) = \ln\left(\sqrt{1+x^2} + x\right) - \frac{\sqrt{1+(x)^2} - 1}{3x} \tag{19}$$

The complex specific acoustic impedance of the system is then calculated in the same process as the infinite case. However, the calculation of the diffuse field absorption coefficient is slightly different (1):

$$\alpha = 8 \int_0^{\frac{\pi}{2}} \cos\theta \sin\theta \frac{Re\left(\frac{Z_{tot}}{\rho_0 c}\right)}{\left|\frac{Z_{tot}}{\rho_0 c} + z_F\right|^2} \frac{1}{\cos\theta}\, d\theta \tag{20}$$

Here, the two $\cos\theta$ values will cancel each other out, resulting in the following equation;

$$\alpha = 8 \int_0^{\frac{\pi}{2}} \sin\theta \frac{Re\left(\frac{Z_{tot}}{\rho_0 c}\right)}{\left|\frac{Z_{tot}}{\rho_0 c} + z_F\right|^2} d\theta \tag{21}$$

The equation can now be solved without problems due to the case when $\theta = \pi/2$.

3. RESULTS

Several thin porous materials have been measured in the two-microphone impedance tube, but only a few have had reverberation room data available for use. In Table 1, three different thin porous materials have been selected to be used in the prediction of diffuse field sound absorption, which range in flow resistance, production and composition.

As shown above in Figure 1, the diffuse field absorption of a particular perforated panel system has been calculated, averaged into third octave bands, and compared to that of measured reverberation room data. Problems arose in the mounting of the thin porous material in the low frequency two-microphone impedance tube, as the sample (100 mm in diameter) is more difficult to have fully taut to prevent a material resonance. When plotted in 4 Hz increments, this particular thin woven material had ripples in the measured values in the results below 500 Hz. While this is not ideal, it still provides reasonable quantitative result. Because the low frequency impedance tube results stop at 1552 Hz, and the high frequency impedance tube results start at 864 Hz, there is an overlap of frequencies. These results are averaged, and fitted into their respective 3rd octave bands.

Less flow resistive materials were also measured to obtain a range of results, where the reverberation room data was already available, as shown in Figure 2. With higher performing systems, the infinite prediction model cannot reach the peak absorption coefficient of the measured data; hence the finite method was also used. However, both models over-predict in the high frequencies, leading to the conclusion that this model is not yet optimized for high performing, bell-shaped curves (where the absorption drops off dramatically each side of the peak); future investigation into improving this model will be needed. Because the measured values lie in between the predicted values, an average can occur to calculate the NRC (Noise Reduction Coefficient), because only over-prediction will occur in the 2000 Hz octave band, which may slightly boost the true NRC value.

Since most perforated panel systems can range in cavity depth, other air cavities had to be explored. In Figure 3, a perforated panel system was predicted with a 400 mm air cavity. In this particular case, the finite model using Equation 21 was the accurate form of prediction across most of the frequency range, even though the infinite model has a very similar shape to the measured data. This shows that these prediction models are suitable for larger air cavity systems, as well as larger perforation ratio panels.

Again it can be seen that over most of the frequency range, the finite prediction model using Equation 21 appears to closest to that of the measured data in terms of values in the mid to high frequencies, but the infinite model has a similar shape to that of the measured data throughout the frequency range. Because the measured data never stated the thickness of the panel, repeated predictions with a change in panel thickness were used to decide on the appropriate thickness. In the process of modeling the Material 3 measurements, the depth of the panel played a significant part in the absorption at the high-end frequency range (4+ kHz). Originally, the panel thickness implemented was 12 mm, and a drop-off in performance can be seen below in Figure 5. This was compared to a higher resistance material (Material 1), which showed the opposite effect in this frequency range.

Due to the material of the perforated panel (steel), it was extremely doubtful that the panel was 12 mm thick, which lead to the change of thickness to 1 mm, and the agreeable results. This was the first perforated panel system that was modeled using a thinner panel, and the first time a drop of absorption performance was recorded. From this, investigation into the perforated panel system performance at the high frequencies was performed.

Ideally, in a perfect situation, the perforated panel system would have a resistance of ~$2\rho_0 c$, and the effective mass of the holes in the material and in the panel would cancel out with the stiffness of the air cavity. Therefore it was originally thought that the lower resistant material would always out-perform the higher resistance material across all frequencies, because of the effect of the perforation ratio factor of the perforated panel on the material. But as shown in Figure 5, this is untrue, especially in the high-end frequency range. Using Equation 12, assuming normal incidence, normalizing the values by dividing the characteristic impedance of air, and rearranging, the calculation of the normalized specific acoustic impedance of the perforated panel z_0 becomes;

$$z_0 = \frac{1}{p}\frac{z_1 + jT}{1 + jz_1T} \tag{22}$$

where $T = \tan(k't)$, and z_1 is the normalized specific acoustic impedance of the addition of the air cavity and the resistive material behind the perforated panel. If z_1 is then broken up into real and imaginary parts (r and x respectively), z_0 becomes;

$$z_0 = \frac{r + j(x + T)}{1 - xT + jrT} \tag{23}$$

$$z_0 = \frac{[r + j(x + T)][(1 - xT) - jrT]}{(1 - xT)^2 + (rT)^2} \tag{24}$$

$$z_0 = \frac{r(1 - xT) + rT(x + T) + j[(x + T)(1 - xT) - r^2T]}{(1 - xT)^2 + (rT)^2} \tag{25}$$

$$z_0 = \frac{r(1 + (T)^2) + j[x - x^2T + T - x(T)^2 - r^2T]}{1 - 2xT + T^2(r^2 + x^2)} \tag{26}$$

The real part of this equation becomes;

$$Re(z_0) = \frac{r(1 + (\tan(k't))^2)}{1 - 2x\tan(k't) + (\tan(k't))^2(r^2 + x^2)} \tag{27}$$

In other words, the resistance of the panel is dependent on the specific acoustic impedance of the air cavity, material resistance and mass. Ideally, the mass of the resistive textile would cancel out with the stiffness of the air cavity, but as this extremely difficult to implement in real circumstances, only the stiffness of the air cavity was used in the values of x.

In Figure 6, the ideal value of the normalized resistance of the system should be close to 2, which lies between the normalized material resistance values of 0.2 and 0.4 for most of the frequency range. However, it can be seen from 2 kHz onwards, that the normalized values of resistance start to interchange with each other, where the least resistant materials effectively dramatically increase the resistance at the high frequencies, which is apparent in Figure 5. To show why the performance of Material 3 did not decreased with a 1 mm thick panel, the

normalized resistance of a 1 mm thick panel was plotted in Figure 7.

As shown above, for a 1 mm thick perforated panel, the resistance stays roughly the same resistance throughout the frequency range, with exception of the resonances of the air cavity. This shows that if perforated panel systems are to be designed to be high performance absorbers over the frequency range of 100 Hz – 6000 Hz, it can be a trade-off between high performance in the low-mid frequency range, and high performance in the high frequency domain. However, frequencies above 2500 Hz do not affect the NRC rating.

Since the NRC is one of the common forms of rating a diffuse field sound absorption system, the measured and predicted NRC values were compared to give a rough idea on how well the predicted values agree with the measured values. The NRC rating involves averaging the diffuse field absorption values across the 250 Hz, 500 Hz, 1 kHz and 2 kHz octave bands. Due to the overlap of frequencies between 864 Hz – 1552 Hz, the predicted diffuse field absorption values were averaged before being used in the calculation of the NRC.

As shown in Table 2, the predicted NRC values are the same or one increment higher or lower than the measured NRC values.

4. CONCLUSIONS

With a range of panel thickness, panel perforation ratio, panel perforation size, thin porous material and air cavity depth, a prediction model of measured diffuse field sound absorption in a reverberation room was implemented, with NRC readings equal to, or one NRC increment either side of the measured NRC values. This model can be used to quantitatively predict the diffuse field sound absorption coefficient. This eliminates the trial and error methods of reverberation room testing of large sample systems.

5. REFERENCES

1. Allard J, Atalla N. “Propagation of Sound in Porous Media: Modelling Sound Absorbing Materials” 2 ed: *Wiley*; (2009).

2. Zwikker C, Kosten CW. “Sound absorbing materials”: *Elsevier Pub. Co.*; (1949).

3. Thomasson S-I. “Theory and experiments on the sounds absorption as function of the area”. *Royal Institute of Technology, Stockholm, Sweden: Royal Institute of Technology*, Contract No.: Report TRITA-TAK 8201. May (1982).

4. Maa DY. “Theory and design of microperforated panel sound-absorbing structures”, *Scientia Sinica*, **18**(1), 55-71, (1975).

5. Maa DY. “Microperforated-panel wideband absorbers”, *Noise Control Engineering Journal*, **29**(3):77-84. Nov-Dec (1987).

6. Maa DY. “Potential of microperforated panel absorber”. *The Journal of the Acoustical Society of America*, **104**(5):2861-6, Nov (1998).

6. APPENDIX

Table 1 – Thin porous materials

Material #	Flow Resistance (Rayl)	Production	Composition
1	746	Woven	
2	273	Woven	
3	243	Matted	Cellulose/Glass

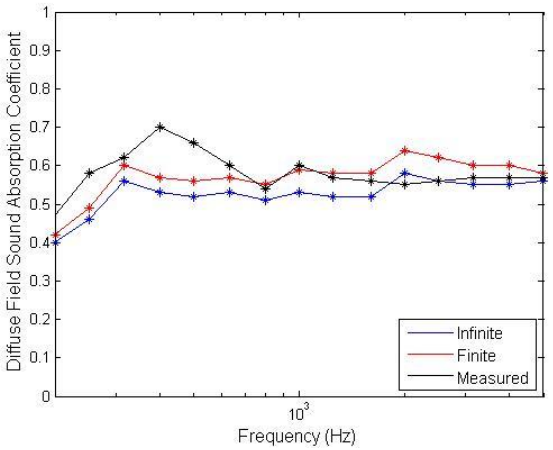

Figure 1 – Diffuse field absorption of a 12 mm thick perforated panel, with 4.5 mm diameter holes and a 0.102 perforation ratio, backed by Material 1 and a 90 mm air cavity. The black line shows the measured reverberation room data, and the red and blue lines show the finite and infinite predictions respectively.

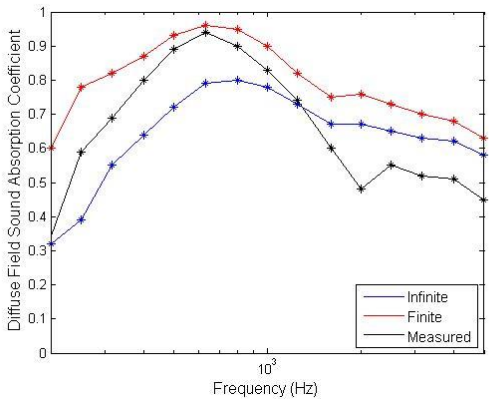

Figure 2 – Diffuse field absorption of a 12 mm thick perforated panel, with 12.7 mm wide slots and a 0.263 perforation ratio, backed by Material 2 and a 90 mm air cavity. The black line shows the measured reverberation room data, and the red and blue lines show the finite and infinite predictions respectively.

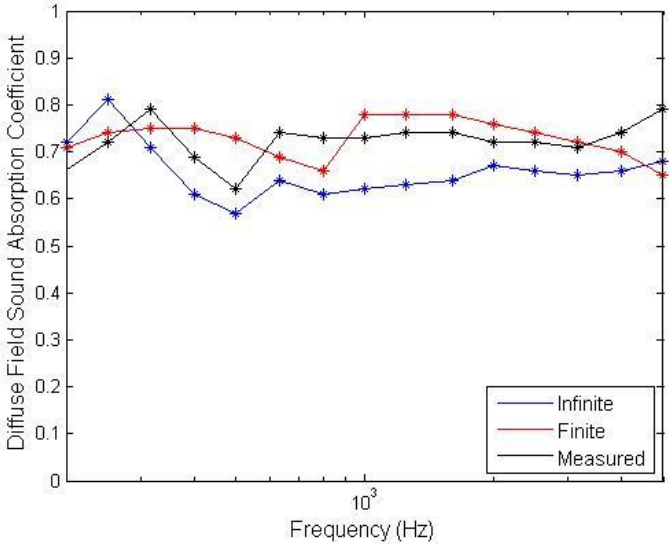

Figure 3 – Diffuse field absorption of a 12 mm thick perforated panel, with 10 mm diameter holes and a 0.251 perforation ratio, backed by Material 1 and a 400 mm air cavity. The black line shows the measured reverberation room data, and the red/magenta and blue lines show the finite and infinite predictions respectively.

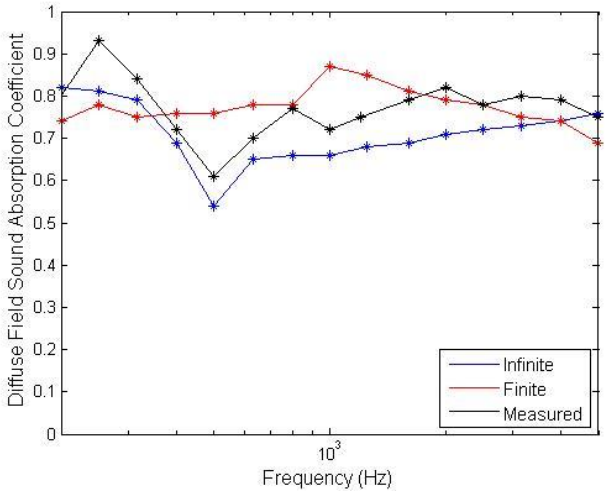

Figure 4 – Diffuse field absorption of a presumed 1 mm thick perforated panel, with 1.8 mm diameter holes, and a 0.2 perforation ratio, backed by Material 3 and a 400 mm air cavity. The black line shows the measured reverberation room data, and the red and blue lines show the finite and infinite predictions respectively.

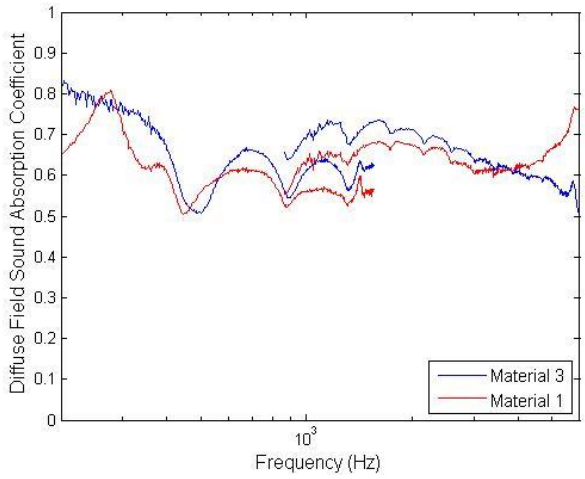

Figure 5 – Diffuse field absorption of a 12 mm thick perforated panel with 1.8 mm diameter holes and a 0.2 perforation ratio, backed by a 400 mm air cavity and either Material 3 (blue) or Material 1 (red).

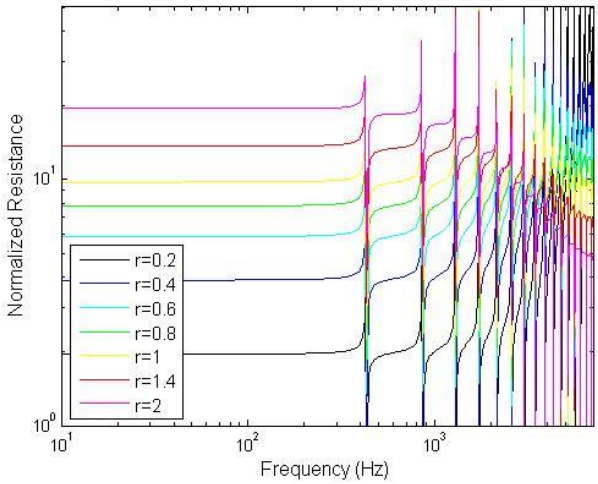

Figure 6 – Normalized resistance $Re(z_0)$ of a 12 mm thick perforated panel with 4.5 mm diameter holes and a perforation ratio of 0.102, backed by a thin porous material and a 400 mm air cavity at normal incidence vs. Frequency.

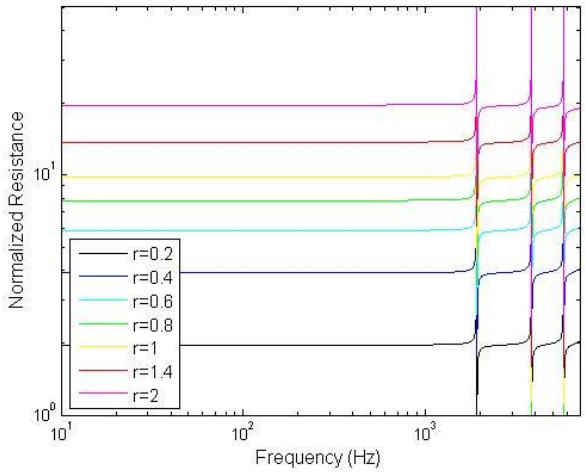

Figure 7 - Normalized resistance $Re(z_0)$ of a 1 mm thick perforated panel with 4.5 mm diameter holes and a perforation ratio of 0.102, backed by a thin porous material and a 90 mm air cavity at normal incidence vs. Frequency

Table 2 – Predicted and Measured NRC values

System	Infinite NRC prediction	Finite NRC prediction	Rounded average predicted NRC	Measured NRC
Figure 1	0.50	0.60	0.55	0.60
Figure 2	0.65	0.80	0.75	0.70
Figure 3	0.65	0.70	0.70	0.70
Figure 4	0.70	0.80	0.75	0.75

The prediction of the diffuse field sound absorption of perforated panel systems

David James Larner[1]
John Laurence Davy[2]
RMIT University
GPO Box 2476
Melbourne, VIC 3001 Australia

This paper studies the diffuse field sound absorption coefficient of a system consisting of a rigid perforated panel with a thin porous woven/matted material glued to its back, which is placed in front of an air cavity with a rigid backing. To cut the cost of trial and error diffuse field sound absorption coefficient measurements, a prediction method was developed. Measurements were made in a two-microphone impedance tube of the complex specific acoustic impedances of the un-perforated rigid panel materials, and of the thin porous materials in front of a rigidly terminated air cavity. These values were used in the transfer matrix method to predict the complex specific acoustic impedances of the perorated panels systems as a function of the angle of incidence of the sound. These calculations assumed the systems to have infinite or finite lateral extent. The measured diffuse field absorption values usually lay between the infinite and finite predictions. The most important variables are the perforation factor of the panel, the acoustic resistance of the thin porous material and the cavity depth.

1. INTRODUCTION

Trial and error can be an expensive task when developing new materials for perforated panel systems. To reduce the cost of diffuse field sound absorption measurements, a prediction method for a system consisting of a rigid perforated panel with a thin porous woven or matted material glued to its back, which is placed in front of an air cavity with a rigid backing, has been developed. The complex specific acoustic impedance of the apertures of the perforated panel was calculated by using predictions of the complex characteristic acoustic impedance and complex wavenumber of the apertures of the perforated panel[1], and using the transfer matrix method[2] to add the impedance of the air cavity. The complex specific acoustic impedance of the thin porous material is added to the complex specific acoustic impedance of

[1] david.larner@rmit.edu.au
[2] john.davy@rmit.edu.au

the air cavity, where the perforation ratio of the panel divides the impedance of the thin porous material.

The complex specific impedance of the panel material is placed in parallel with the complex specific impedance of the system, as this material can be absorptive. The infinite radiation impedance was originally used to predict the diffuse field sound absorption. However, this usually under-predicts compared to the measured values. Therefore, the finite radiation impedance was used in the calculation of the diffuse field sound absorption[3]. This method over-predicts the measured values, which means that the average between the infinite and finite analysis can be used as an estimate of the diffuse field sound absorption coefficient.

2. THEORY

2.1 Infinite calculation of the diffuse field sound absorption

Perforated panels have been used as Helmholtz resonators in the sound absorption industry for a number of years. After studying the micro-perforated theory[4-6], the development of a method to predict the diffuse field sound absorption coefficient α of a much thicker panel was instigated. Since the transfer matrix method is used, the specific acoustic impedance of the rigidly terminated air cavity at the back of the holes in the perforated panel needs to be calculated first;

$$Z_{cav} = -jp\rho_0 c \cot(kD\cos\theta) / \cos\theta \quad (1)$$

where p is the perforation ratio of the panel, $\rho_0 c$ is the characteristic impedance of air, k is the wavenumber of air, D is the air cavity depth, and θ is the angle of incidence. The reason for the multiplication of the perforation ratio here is the difference between the acoustic particle velocity inside and outside the holes.

Here, the measured complex specific acoustic impedance of the thin porous material Z_{woven} is added to the impedance of the air cavity.

$$Z_1 = Z_{woven} + Z_{cav} \quad (2)$$

This measurement is performed in both a low frequency and a high frequency two-microphone impedance tube, so a wide range of frequencies are measured (172 – 5936 Hz). This was performed by gluing the material to a metal mount, so the thin porous material is free standing, roughly one-quarter wavelength of the maximum frequency away from the rigid backing. This quarter wavelength-sized air cavity is then subtracted from the measurements, so the complex specific acoustic impedance of the material is solely added to the theoretical air cavity depth.

Before the transfer matrix method is used, the complex characteristic impedance and complex wavenumber of the perforated panel needs to be calculated. These values are calculated using the effective density ρ_e and the bulk modulus K. For circular apertures, the bulk modulus (at 18°C) can be calculated by;

$$K_{cir} = \gamma P_o / \left[1 + (\gamma - 1)\frac{2}{Bs\sqrt{-j}}\frac{J_1(Bs\sqrt{-j})}{J_0(Bs\sqrt{-j})}\right] \quad (3)$$

where γ is the diatomic adiabatic constant, P_o is the ambient mean pressure, B is the square root of the Prandtl number ($\sqrt{0.71}$), and J_n is the nth order Bessel function of the first kind. s is equal to;

$$s = \sqrt{\frac{\omega \rho_0 R^2}{\eta}} \quad (4)$$

where ω is the angular frequency, ρ_0 is the density of air, R is the radius of the aperture, and η is the viscosity of air.

These previous two equations can be modified for slits;

$$K_{slit} = \gamma P_o / \left[1 + (\gamma - 1)\frac{\tanh(Bs\prime\sqrt{j})}{Bs\prime\sqrt{j}}\right] \quad (5)$$

$$s' = \sqrt{\frac{\omega \rho_0 a^2}{\eta}} \quad (6)$$

where a is the width of the slit.

The effective density is then calculated, for both circular apertures $\rho_{e_{cir}}$ and slits $\rho_{e_{slit}}$ respectively;

$$\rho_{e_{cir}} = \rho_0 / \left[1 - \frac{2}{s\sqrt{-j}}\frac{J_1(s\sqrt{-j})}{J_0(s\sqrt{-j})}\right] \quad (7)$$

$$\rho_{e_{slit}} = \rho_0 / \left[1 - \frac{\tanh(s\prime\sqrt{j})}{s\prime\sqrt{j}}\right] \quad (8)$$

From these calculations, the complex characteristic impedance Z_c and complex wavenumber k' of the perforated panel can be calculated;

$$Z_c = \sqrt{K\rho_e} \quad (9)$$

$$k' = \omega\sqrt{\rho_e / K} \quad (10)$$

There needs to be an angular dependent term when calculating the specific acoustic impedance of the apertures in the perforated panel. This is obtained when calculating the component of the vector of the complex wavenumber transmitting in the plane perpendicular to the face of the panel k'_3;

$$k'_3 = \sqrt{k'^2 - {k_0}^2 \sin^2(\theta)} \quad (11)$$

With these values, the specific acoustic impedance of the apertures in the panel Z_0 can now be calculated;

$$Z_0 = \frac{Z_c}{p}\frac{k'}{k'_3}\frac{-jZ_1\cot(k'_3 t) + Z_c\frac{k'}{k'_3}}{Z_1 - jZ_c\frac{k'}{k'_3}\cot(k'_3 t)} \tag{12}$$

where t is the thickness of the panel. To obtain the total impedance of the system, the material impedance of the panel needs to be incorporated into the system. This was performed by first measuring the complex specific acoustic impedance of an un-perforated version of the panel Z_{panel}, rigidly-backed, in the two-microphone impedance tube. These measurements were then used in parallel with the aperture impedances, to give the total impedance of the system;

$$Z_{tot} = \left(\frac{1}{Z_0} + \frac{1-p}{Z_{panel}}\right)^{-1} \tag{13}$$

The diffuse field sound absorption coefficient can then be calculated for the entire system using the commonly found equation;

$$\alpha = 8\int_0^{\frac{\pi}{2}} \sin\theta\cos\theta \frac{Re\left(\frac{Z_{tot}}{\rho_0 c}\right)\cos\theta}{\left[1 + Re\left(\frac{Z_{tot}}{\rho_0 c}\right)\cos\theta\right]^2 + \left[Im\left(\frac{Z_{tot}}{\rho_0 c}\right)\cos\theta\right]^2} d\theta \tag{14}$$

2.2 Finite calculation of the diffuse field absorption

Finite analysis was also used to calculate the diffuse field sound absorption coefficient, as this method tends to boost the diffuse field sound absorption coefficient values across all frequencies. This was performed by calculating the normalized complex finite radiation impedance[3]. Firstly, the real part of the normalized finite radiation impedance must be calculated:

$$Re(z_F) = \left[Re\left(z_{F_H}\right)^{-2} + \left(\frac{{k_0}^2 A}{2\pi}\right)^{-2}\right]^{-\frac{1}{2}} \tag{15}$$

where A is the area of the perforated panel, and the high frequency approximation of the normalized finite impedance z_{F_H} is;

$$z_{F_H} = \sqrt{\left(\cos^2\theta + \left[\frac{\beta(L+W)}{Ak_0}\right]^2 - 2j\frac{\beta(L+W)}{Ak_0}\sin\theta\right)^{-1}} \tag{16}$$

where L and W are the length and width of the perforated panel respectively, and $\beta = 0.956$.

The imaginary part of the normalized radiation impedance is calculated by;

$$Im(z_F) = \begin{cases} z_{F_0} & if\ z_{F_0} > Im(z_{F_H}) \\ Im(z_{F_H}) & if\ \ z_{F_0} < Im(z_{F_H}) \end{cases} \tag{17}$$

where;

$$z_{F_0} = \left[\left(\frac{k_0 \left[WH\left(\frac{L}{W}\right) + L\,H\left(\frac{W}{L}\right) \right]}{\pi} \right)^{-2} + \left(\frac{0.67(L+W)}{k_0 A} \right)^{-2} \right]^{-\frac{1}{2}} \tag{18}$$

and;

$$H(x) = \ln\left(\sqrt{1+x^2} + x\right) - \frac{\sqrt{1+(x)^2} - 1}{3x} \tag{19}$$

The complex specific acoustic impedance of the system is then calculated in the same process as the infinite case. However, the calculation of the diffuse field absorption coefficient is slightly different (1):

$$\alpha = 8 \int_0^{\frac{\pi}{2}} \cos\theta \sin\theta \frac{Re\left(\frac{Z_{tot}}{\rho_0 c}\right)}{\left|\frac{Z_{tot}}{\rho_0 c} + z_F\right|^2} \frac{1}{\cos\theta}\, d\theta \tag{20}$$

Here, the two $\cos\theta$ values will cancel each other out, resulting in the following equation;

$$\alpha = 8 \int_0^{\frac{\pi}{2}} \sin\theta \frac{Re\left(\frac{Z_{tot}}{\rho_0 c}\right)}{\left|\frac{Z_{tot}}{\rho_0 c} + z_F\right|^2} d\theta \tag{21}$$

The equation can now be solved without problems due to the case when $\theta = \pi/2$.

3. RESULTS

Several thin porous materials have been measured in the two-microphone impedance tube, but only a few have had reverberation room data available for use. In Table 1, three different thin porous materials have been selected to be used in the prediction of diffuse field sound absorption, which range in flow resistance, production and composition.

As shown above in Figure 1, the diffuse field absorption of a particular perforated panel system has been calculated, averaged into third octave bands, and compared to that of measured reverberation room data. Problems arose in the mounting of the thin porous material in the low frequency two-microphone impedance tube, as the sample (100 mm in diameter) is more difficult to have fully taut to prevent a material resonance. When plotted in 4 Hz increments, this particular thin woven material had ripples in the measured values in the results below 500 Hz. While this is not ideal, it still provides reasonable quantitative result. Because the low frequency impedance tube results stop at 1552 Hz, and the high frequency impedance tube results start at 864 Hz, there is an overlap of frequencies. These results are averaged, and fitted into their respective 3rd octave bands.

Less flow resistive materials were also measured to obtain a range of results, where the reverberation room data was already available, as shown in Figure 2. With higher performing systems, the infinite prediction model cannot reach the peak absorption coefficient of the measured data; hence the finite method was also used. However, both models over-predict in the high frequencies, leading to the conclusion that this model is not yet optimized for high performing, bell-shaped curves (where the absorption drops off dramatically each side of the peak); future investigation into improving this model will be needed. Because the measured values lie in between the predicted values, an average can occur to calculate the NRC (Noise Reduction Coefficient), because only over-prediction will occur in the 2000 Hz octave band, which may slightly boost the true NRC value.

Since most perforated panel systems can range in cavity depth, other air cavities had to be explored. In Figure 3, a perforated panel system was predicted with a 400 mm air cavity. In this particular case, the finite model using Equation 21 was the accurate form of prediction across most of the frequency range, even though the infinite model has a very similar shape to the measured data. This shows that these prediction models are suitable for larger air cavity systems, as well as larger perforation ratio panels.

Again it can be seen that over most of the frequency range, the finite prediction model using Equation 21 appears to closest to that of the measured data in terms of values in the mid to high frequencies, but the infinite model has a similar shape to that of the measured data throughout the frequency range. Because the measured data never stated the thickness of the panel, repeated predictions with a change in panel thickness were used to decide on the appropriate thickness. In the process of modeling the Material 3 measurements, the depth of the panel played a significant part in the absorption at the high-end frequency range (4+ kHz). Originally, the panel thickness implemented was 12 mm, and a drop-off in performance can be seen below in Figure 5. This was compared to a higher resistance material (Material 1), which showed the opposite effect in this frequency range.

Due to the material of the perforated panel (steel), it was extremely doubtful that the panel was 12 mm thick, which lead to the change of thickness to 1 mm, and the agreeable results. This was the first perforated panel system that was modeled using a thinner panel, and the first time a drop of absorption performance was recorded. From this, investigation into the perforated panel system performance at the high frequencies was performed.

Ideally, in a perfect situation, the perforated panel system would have a resistance of ~$2\rho_0 c$, and the effective mass of the holes in the material and in the panel would cancel out with the stiffness of the air cavity. Therefore it was originally thought that the lower resistant material would always out-perform the higher resistance material across all frequencies, because of the effect of the perforation ratio factor of the perforated panel on the material. But as shown in Figure 5, this is untrue, especially in the high-end frequency range. Using Equation 12, assuming normal incidence, normalizing the values by dividing the characteristic impedance of air, and rearranging, the calculation of the normalized specific acoustic impedance of the perforated panel z_0 becomes;

$$z_0 = \frac{1}{p}\frac{z_1 + jT}{1 + jz_1T} \tag{22}$$

where $T = \tan(k't)$, and z_1 is the normalized specific acoustic impedance of the addition of the air cavity and the resistive material behind the perforated panel. If z_1 is then broken up into real and imaginary parts (r and x respectively), z_0 becomes;

$$z_0 = \frac{r + j(x + T)}{1 - xT + jrT} \tag{23}$$

$$z_0 = \frac{[r + j(x + T)][(1 - xT) - jrT]}{(1 - xT)^2 + (rT)^2} \tag{24}$$

$$z_0 = \frac{r(1 - xT) + rT(x + T) + j[(x + T)(1 - xT) - r^2T]}{(1 - xT)^2 + (rT)^2} \tag{25}$$

$$z_0 = \frac{r(1 + (T)^2) + j[x - x^2T + T - x(T)^2 - r^2T]}{1 - 2xT + T^2(r^2 + x^2)} \tag{26}$$

The real part of this equation becomes;

$$Re(z_0) = \frac{r(1 + (\tan(k't))^2)}{1 - 2x\tan(k't) + (\tan(k't))^2(r^2 + x^2)} \tag{27}$$

In other words, the resistance of the panel is dependent on the specific acoustic impedance of the air cavity, material resistance and mass. Ideally, the mass of the resistive textile would cancel out with the stiffness of the air cavity, but as this extremely difficult to implement in real circumstances, only the stiffness of the air cavity was used in the values of x.

In Figure 6, the ideal value of the normalized resistance of the system should be close to 2, which lies between the normalized material resistance values of 0.2 and 0.4 for most of the frequency range. However, it can be seen from 2 kHz onwards, that the normalized values of resistance start to interchange with each other, where the least resistant materials effectively dramatically increase the resistance at the high frequencies, which is apparent in Figure 5. To show why the performance of Material 3 did not decreased with a 1 mm thick panel, the

normalized resistance of a 1 mm thick panel was plotted in Figure 7.

As shown above, for a 1 mm thick perforated panel, the resistance stays roughly the same resistance throughout the frequency range, with exception of the resonances of the air cavity. This shows that if perforated panel systems are to be designed to be high performance absorbers over the frequency range of 100 Hz – 6000 Hz, it can be a trade-off between high performance in the low-mid frequency range, and high performance in the high frequency domain. However, frequencies above 2500 Hz do not affect the NRC rating.

Since the NRC is one of the common forms of rating a diffuse field sound absorption system, the measured and predicted NRC values were compared to give a rough idea on how well the predicted values agree with the measured values. The NRC rating involves averaging the diffuse field absorption values across the 250 Hz, 500 Hz, 1 kHz and 2 kHz octave bands. Due to the overlap of frequencies between 864 Hz – 1552 Hz, the predicted diffuse field absorption values were averaged before being used in the calculation of the NRC.

As shown in Table 2, the predicted NRC values are the same or one increment higher or lower than the measured NRC values.

4. CONCLUSIONS

With a range of panel thickness, panel perforation ratio, panel perforation size, thin porous material and air cavity depth, a prediction model of measured diffuse field sound absorption in a reverberation room was implemented, with NRC readings equal to, or one NRC increment either side of the measured NRC values. This model can be used to quantitatively predict the diffuse field sound absorption coefficient. This eliminates the trial and error methods of reverberation room testing of large sample systems.

5. REFERENCES

1. Allard J, Atalla N. “Propagation of Sound in Porous Media: Modelling Sound Absorbing Materials” 2 ed: *Wiley*; (2009).

2. Zwikker C, Kosten CW. “Sound absorbing materials”: *Elsevier Pub. Co.*; (1949).

3. Thomasson S-I. “Theory and experiments on the sounds absorption as function of the area”. *Royal Institute of Technology, Stockholm, Sweden: Royal Institute of Technology*, Contract No.: Report TRITA-TAK 8201. May (1982).

4. Maa DY. “Theory and design of microperforated panel sound-absorbing structures”, *Scientia Sinica*, **18**(1), 55-71, (1975).

5. Maa DY. “Microperforated-panel wideband absorbers”, *Noise Control Engineering Journal*, **29**(3):77-84. Nov-Dec (1987).

6. Maa DY. “Potential of microperforated panel absorber”. *The Journal of the Acoustical Society of America*, **104**(5):2861-6, Nov (1998).

6. APPENDIX

Table 1 – Thin porous materials

Material #	Flow Resistance (Rayl)	Production	Composition
1	746	Woven	
2	273	Woven	
3	243	Matted	Cellulose/Glass

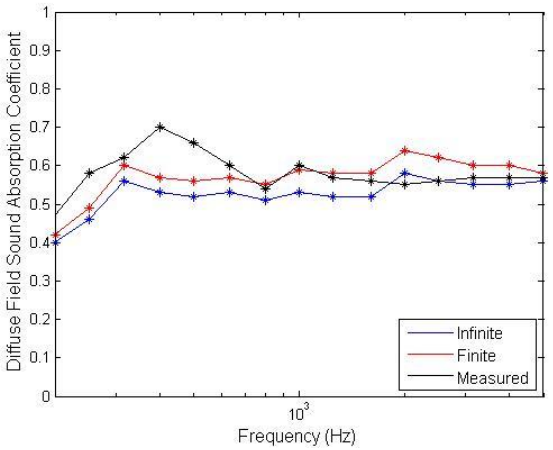

Figure 1 – Diffuse field absorption of a 12 mm thick perforated panel, with 4.5 mm diameter holes and a 0.102 perforation ratio, backed by Material 1 and a 90 mm air cavity. The black line shows the measured reverberation room data, and the red and blue lines show the finite and infinite predictions respectively.

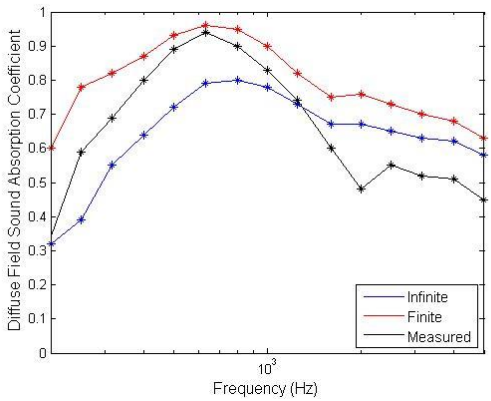

Figure 2 – Diffuse field absorption of a 12 mm thick perforated panel, with 12.7 mm wide slots and a 0.263 perforation ratio, backed by Material 2 and a 90 mm air cavity. The black line shows the measured reverberation room data, and the red and blue lines show the finite and infinite predictions respectively.

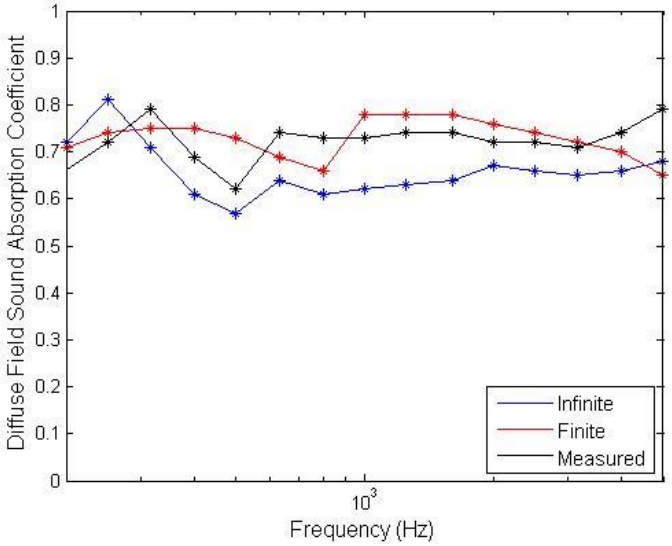

Figure 3 – Diffuse field absorption of a 12 mm thick perforated panel, with 10 mm diameter holes and a 0.251 perforation ratio, backed by Material 1 and a 400 mm air cavity. The black line shows the measured reverberation room data, and the red/magenta and blue lines show the finite and infinite predictions respectively.

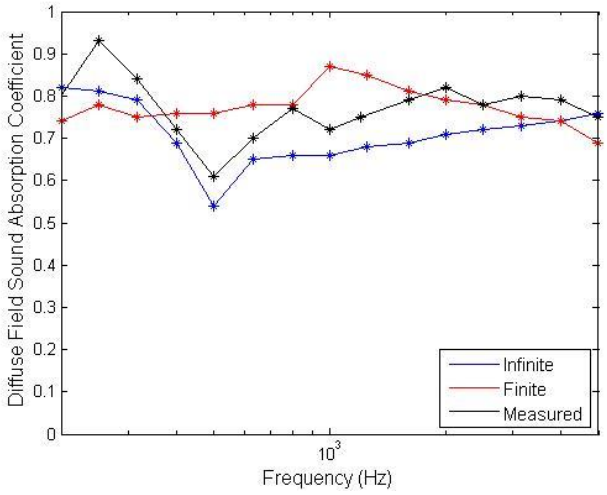

Figure 4 – Diffuse field absorption of a presumed 1 mm thick perforated panel, with 1.8 mm diameter holes, and a 0.2 perforation ratio, backed by Material 3 and a 400 mm air cavity. The black line shows the measured reverberation room data, and the red and blue lines show the finite and infinite predictions respectively.

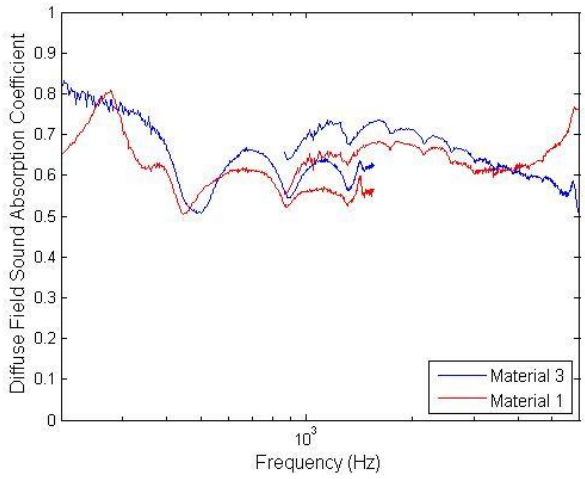

Figure 5 – Diffuse field absorption of a 12 mm thick perforated panel with 1.8 mm diameter holes and a 0.2 perforation ratio, backed by a 400 mm air cavity and either Material 3 (blue) or Material 1 (red).

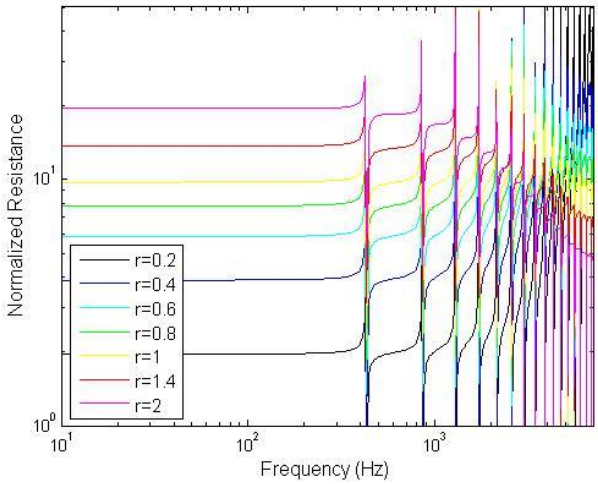

Figure 6 – Normalized resistance $Re(z_0)$ of a 12 mm thick perforated panel with 4.5 mm diameter holes and a perforation ratio of 0.102, backed by a thin porous material and a 400 mm air cavity at normal incidence vs. Frequency.

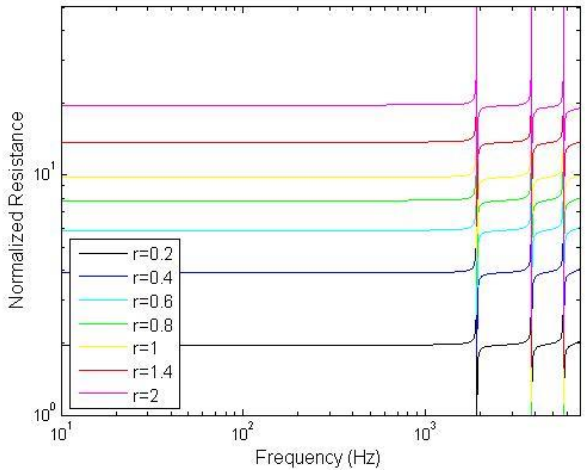

Figure 7 - Normalized resistance $Re(z_0)$ of a 1 mm thick perforated panel with 4.5 mm diameter holes and a perforation ratio of 0.102, backed by a thin porous material and a 90 mm air cavity at normal incidence vs. Frequency

Table 2 – Predicted and Measured NRC values

System	Infinite NRC prediction	Finite NRC prediction	Rounded average predicted NRC	Measured NRC
Figure 1	0.50	0.60	0.55	0.60
Figure 2	0.65	0.80	0.75	0.70
Figure 3	0.65	0.70	0.70	0.70
Figure 4	0.70	0.80	0.75	0.75